

Virtual photons in the pion form factors and the energy–momentum tensor

Bastian Kubis,^{#1} Ulf-G. Meißner^{#2}

*Forschungszentrum Jülich, Institut für Kernphysik (Theorie)
D-52425 Jülich, Germany*

Abstract

We evaluate the vector and scalar form factor of the pion in the presence of virtual photons at next-to-leading order in two-flavor chiral perturbation theory. We also consider the scalar and tensor pion form factors of the energy–momentum tensor. We find that the intrinsic electromagnetic corrections are of the expected size for the vector form factor and very small for the charged pion scalar form factor. Detector resolution independent photon corrections reduce the vector radius by about one percent. The scalar radius of the neutral pion is reduced by two percent by isospin–breaking contributions. We perform infrared regularization by considering electron–positron annihilation into pions and the decay of a light Higgs boson into a pion pair. We discuss the detector resolution dependent contributions to the various form factors and pion radii.

PACS: 12.39.Fe, 13.40.Gp, 13.40.Ks, 14.40.Aq

Keywords: *Pion form factors, chiral perturbation theory, energy–momentum tensor*

^{#1}email: b.kubis@fz-juelich.de

^{#2}email: Ulf-G.Meissner@fz-juelich.de

1 Introduction

In their seminal paper of 1984, Gasser and Leutwyler [1] set up the scheme to investigate the consequences of the broken chiral symmetry of QCD in a systematic fashion. This method is called chiral perturbation theory (CHPT) and rests on the fact that at low energies, the (pseudo)Goldstone bosons (the pions) interact weakly and saturate most n -point functions almost completely. The underlying power counting and an outline of the method had already been established by Weinberg in 1979 [2]. In ref. [1], a whole series of applications was considered to one-loop accuracy (next-to-leading order), like e.g. the vector and scalar form factor of the pion, elastic pion-pion scattering, pion radiative decay and so on. By now, all of the observables and processes considered in [1] have been worked out to two-loop accuracy, either by direct Feynman graph calculations or by making use of dispersive methods.^{#3} We mention here the pion mass and decay constant [3], the pion form factors [4, 5], and $\pi\pi$ scattering [6, 7]. In most cases these two-loop corrections are sizeably smaller than the corresponding one-loop terms, as expected by the power counting underlying CHPT. We remark that the improved two-loop representation of the vector form factor of the pion has been used to significantly decrease the hadronic uncertainty for the muon ($g - 2$) prediction [8]. In addition, there is a series of upcoming experiments to pin down precisely the $\pi\pi$ S-wave scattering lengths (via K_{l4} decays at BNL and DAΦNE or pionium lifetime measurements at CERN). However, as first pointed out in ref. [9] and further quantified in ref. [10], electromagnetic corrections to elastic $\pi\pi$ -scattering in the threshold region are of the same size as the hadronic two-loop contributions. At the level of the presently achieved accuracy, it is therefore mandatory to include virtual photons and work out the dual effects of isospin violation due to the light quark mass difference and the electromagnetic interaction. This machinery was essentially started in refs. [11, 12, 13] for the three flavor case in connection with the violation of Dashen's theorem (see also ref. [14]), which is of importance for extracting the quark mass ratios from the masses of the Goldstone bosons.

Here, we will be concerned with the vector and scalar form factor of the pion as well as pionic matrix elements of the energy-momentum tensor in the presence of virtual photons. The scalar form factor is of interest for various reasons. Due to its quantum numbers, its phase is related to the strong $\pi\pi$ interaction in the isospin zero S-wave and it also exhibits the unitary cusp at the opening of the two-pion threshold. Furthermore, it gives a direct measure of the QCD quark mass term in the pion. In addition, the scalar form factor plays an essential role in the dispersive analysis of the so-called pion-nucleon σ -term, which allows one to extract information about the strangeness component in the nucleon wave function. In the pion-nucleon sector, isoscalar quantities can be very sensitive to strong and/or electromagnetic isospin breaking, see e.g. [15, 16, 17, 18]. It is therefore mandatory to evaluate the effects of virtual photons on this scalar-isoscalar quantity. Similarly, the hadronic two-loop representation of the vector form factor is extremely precise and has even been used to extract the pion charge radius from space- and time-like data at low energies [5].

^{#3}Note that using dispersive methods does in general not allow to study the quark mass dependence of observables.

Here, the celebrated Ademollo–Gatto theorem [19] lets one expect that symmetry breaking corrections are fairly small, but their precise magnitude has so far not been worked out. Another set of form factors is related to the pion matrix elements of the energy–momentum tensor [20], which play a role in the decay of a light Higgs into two pions [21, 22] or heavy quarkonia transitions into the ground state with the emission of a pion pair. Of particular interest is the trace of the energy–momentum tensor which allows one to study the interplay of conformal and chiral symmetry [23] or the hadron mass composition [24]. Clearly, it is of interest to learn about the modifications induced by virtual photons, although we expect these to be small effects.

Of course, whenever one deals with virtual photons, one encounters infrared (IR) singularities due to the vanishing photon mass. These divergences can be cured by taking into account the effects of radiation of soft photons which have an energy below a given detector resolution. For that, one has to consider cross sections or decay widths. In our case, we consider the squares of the corresponding form factors since that is the way they appear in the pertinent cross sections or decay rates. For the vector form factor, we consider the process $e^+e^- \rightarrow \pi^+\pi^-$. The less easily accessible scalar form factor together with the form factor of the trace anomaly can be studied in the decay of the Higgs boson into two pions. We note that to the order we are working, we have to consider only the radiation of exactly one soft photon from any one of the final–state pion legs. Radiation of two or more soft photons is of higher order in the fine structure constant.

The paper is organized as follows. In sect. 2 we briefly discuss the strong and electromagnetic effective chiral Lagrangians underlying our calculation. We work in $SU(2)$ and to fourth order in the chiral expansion, counting the electric charge e as a small parameter like external momenta or pion mass insertions. In sect. 3 we give the results for the scalar and vector form factor of the pion at next–to–leading order including virtual photons and discuss the various checks on our calculation. The infrared regularization is performed by means of a finite photon mass. In sect. 4 we briefly review the effective Lagrangian for pions and external fields coupled to gravity and include virtual photons. The pion matrix elements of the energy–momentum tensor are calculated in sect. 5 to fourth order in the chiral expansion including virtual photons and compared with previous results (obtained in the isospin limit). The problem of infrared regularization is taken up in sect. 6. Our results are presented and discussed in sect. 7. A short summary is given in sect. 8.

2 Effective Lagrangian with pions and virtual photons

In this section we discuss the strong and electromagnetic effective Lagrangians underlying our calculations. The various pieces have already been discussed in the literature, so we will be brief and just collect the terms actually needed in what follows. The effective Lagrangian has the energy expansion

$$\mathcal{L}_{\text{eff}} = \mathcal{L}^{(2,\text{str})} + \mathcal{L}^{(4,\text{str})} + \mathcal{L}^{(2,\text{em})} + \mathcal{L}^{(4,\text{em})} + \dots, \quad (2.1)$$

where the superscripts 2, 4 refer to the chiral dimension and “str” and “em” denote the strong and the electromagnetic terms, respectively. The ellipsis stands for higher order terms not considered here. Our power counting is based on the observation that $e^2/4\pi \simeq M_\pi^2/(4\pi F)^2 \simeq 1/100$, with M_π the pion mass and F the weak pion decay constant. This means that we consider the electric charge as a small parameter similar to the external momenta and pion mass insertions. Consequently, any term of the form $e^{2n} q^{2m} M_\pi^{2l}$ with $n+m+l = 2$ is counted as fourth order. In what follows, we denote such a term as $\mathcal{O}(q^4)$ without differentiating between external momenta, pion mass insertions, or powers of the electric charge.

At leading order, the strong Lagrangian is nothing but the non-linear σ -model coupled to external sources,

$$\mathcal{L}^{(2,\text{str})} = \frac{F^2}{4} \langle u_\mu u^\mu + \chi_+ \rangle, \quad (2.2)$$

where $\langle \dots \rangle$ denotes the trace in flavor space, $U(x) = u^2(x)$ parametrizes the pion fields, $u_\mu = iu^\dagger D_\mu U u^\dagger$ is the conventional pion viel-bein and D_μ the chiral covariant derivative in the presence of external vector and axial-vector fields. Furthermore, $\chi = 2B_0(s + ip)$ subsumes the external scalar and pseudoscalar sources, and $\chi_+ = u^\dagger \chi u^\dagger + u \chi^\dagger u$. The external scalar source contains the quark mass matrix, $s(x) = \text{diag}(m_u, m_d) + \dots$, and $B_0 = |\langle 0 | \bar{q}q | 0 \rangle| / F^2$ measures the strength of the spontaneous symmetry breaking. We assume $B_0 \gg F$ (standard CHPT). Throughout, we work in the so-called σ -model gauge, which simplifies the calculations. It is given by

$$U(x) = \sigma(x) \mathbf{1}_2 + i \vec{\tau} \cdot \vec{\pi}(x) / F, \quad \sigma(x) = \sqrt{1 - \pi^2(x) / F^2}, \quad (2.3)$$

with $\mathbf{1}_2$ the unit matrix in flavor space. The relevant terms of the strong Lagrangian at next-to-leading order read (we use the notation of ref. [25])

$$\mathcal{L}^{(4,\text{str})} = \frac{l_3}{16} \langle \chi_+ \rangle^2 + \frac{i l_4}{4} \langle u_\mu \chi_- \rangle + \frac{i l_6}{4} \langle f_+^{\mu\nu} [u_\mu, u_\nu] \rangle - \frac{l_7}{16} \langle \chi_- \rangle^2, \quad (2.4)$$

with $\chi_- = u^\dagger \chi u^\dagger - u \chi^\dagger u$, $\chi_-^\mu = u^\dagger D^\mu \chi u^\dagger - u D^\mu \chi^\dagger u$, $f_+^{\mu\nu} = u F_{\mu\nu} u^\dagger + u^\dagger F_{\mu\nu} u$, and $F_{\mu\nu} = \partial_\mu A_\nu - \partial_\nu A_\mu$ is the conventional photon field strength tensor. The low energy constants (LECs) l_3 and l_4 appear in the chiral expansion of the pion mass and pion decay constant (and thus in the scalar form factor), whereas l_6 features prominently in the pion charge radius as discussed below. Of particular interest to us is the term $\sim l_7$ since it embodies the strong isospin violation $\sim (m_d - m_u)$. After standard renormalization, the l_i turn into scale-dependent, renormalized LECs called $l_i^r(\lambda)$. As first proposed in ref. [1], we work instead with scale-independent LECs \bar{l}_i obtained from the $l_i^r(\lambda)$ via

$$l_i^r(\lambda) = \frac{\beta_i}{32\pi^2} \left[\bar{l}_i + \log \frac{M_{\pi^0}^2}{\lambda^2} \right], \quad (2.5)$$

with λ the scale of dimensional regularization and β_i the pertinent β -functions. We remark that we use the neutral pion mass as the reference scale since the charged to neutral pion mass difference is almost entirely of electromagnetic origin. Note that l_7 does not get renormalized

($\beta_7 = 0$) and in that case we simply set $\bar{l}_7 = 16\pi^2 l_7$. This procedure is adopted for all other counterterms with vanishing β -functions. The numerical values of the LECs will be given later.

The leading order electromagnetic Lagrangian reads [14]

$$\mathcal{L}^{(2,\text{em})} = -\frac{1}{4}F_{\mu\nu}F^{\mu\nu} - \frac{1}{2a}(\partial \cdot A)^2 + C \langle QUQU^\dagger \rangle, \quad (2.6)$$

with $Q = \text{diag}(2/3, -1/3)$ the quark charge matrix and a the gauge fixing parameter. In what follows, we work in the Feynman gauge $a = 1$.^{#4} In the σ -model gauge for the pions, the last term of this Lagrangian leads only to a term quadratic in pion fields. Consequently, the LEC C can be calculated from the charged to neutral pion mass difference,

$$(M_{\pi^\pm}^2 - M_{\pi^0}^2)_{\text{em}} = (\delta M_\pi^2)_{\text{em}} = \frac{2e^2 C}{F^2} = 2Z e^2 F^2, \quad Z = \frac{C}{F^4}. \quad (2.7)$$

We have $Z = 0.89$ if we use for F its value in the chiral limit, $F_0 = 88 \text{ MeV}$. At next-to-leading order, the relevant terms from the electromagnetic Lagrangian read [13, 9, 10]

$$\begin{aligned} \mathcal{L}^{(4,\text{em})} = & k_1 F^4 \langle QUQU^\dagger \rangle^2 + k_2 F^2 \langle QUQU^\dagger \rangle \langle D_\mu U D^\mu U^\dagger \rangle \\ & + k_3 F^2 (\langle U^\dagger D_\mu U Q \rangle^2 + \langle D_\mu U U^\dagger Q \rangle^2) + k_4 F^2 \langle U^\dagger D_\mu U Q \rangle \langle D_\mu U U^\dagger Q \rangle \\ & + k_7 F^2 \langle QUQU^\dagger \rangle \langle \chi U^\dagger + U \chi^\dagger \rangle + k_8 F^2 \langle (U^\dagger \chi - \chi^\dagger U) (U^\dagger Q U Q - Q U^\dagger Q U) \rangle \\ & + k_9 F^4 \langle Q^2 \rangle \langle QUQU^\dagger \rangle + k_{10} F^2 \langle Q^2 \rangle \langle D_\mu U D^\mu U^\dagger \rangle + k_{11} F^2 \langle Q^2 \rangle \langle \chi U^\dagger + U \chi^\dagger \rangle \\ & + k_{14} F^2 \langle (\chi U^\dagger + U \chi^\dagger) Q + (\chi^\dagger U + U^\dagger \chi) Q \rangle \langle Q \rangle. \end{aligned} \quad (2.8)$$

Note that the covariant derivative D_μ contains external vector sources and the virtual photon fields, see e.g. refs. [13, 9]. The terms proportional to k_1 and k_9 are only needed for the mass renormalization of the charged pions and the trace of the energy-momentum tensor (as discussed below). For estimates of some of the LECs k_i needed in connection with the violation of Dashen's theorem, see refs. [26, 27]. As shown in ref. [10], one needs additional divergent terms in the one-loop generating functional to renormalize the photon propagator,

$$\mathcal{Z}_{1\text{-loop}}^{(\text{em},\gamma)} = -\frac{1}{(4\pi)^2 \epsilon} \int d^4 x \left(-\frac{1}{6} \langle G_{\mu\nu}^R U G^{L,\mu\nu} U^\dagger \rangle - \frac{1}{12} \langle G_{\mu\nu}^R G^{R,\mu\nu} + G_{\mu\nu}^L G^{L,\mu\nu} \rangle + \frac{1}{6} \langle Q \rangle^2 F_{\mu\nu} F^{\mu\nu} \right), \quad (2.9)$$

(where $\epsilon = d - 4$) in terms of left/right-handed gauge fields (for more precise definitions, we refer to app. A of ref. [10]). In our case, we can substitute $G_{\mu\nu}^{R,L}$ by $Q F_{\mu\nu}$ and set $U(x) = 1$. Thus, eq. (2.9) boils down to one term of the form

$$\mathcal{L}^{(4,\text{em},\gamma)} = -\frac{k_\gamma}{4} e^2 F_{\mu\nu} F^{\mu\nu}, \quad (2.10)$$

with the corresponding β -function being $\beta_\gamma = 2/3$. From that, one easily deduces the Z -factor of the photon,

$$Z_\gamma = 1 + \left(\frac{e}{4\pi} \right)^2 \frac{1}{3} (\bar{k}_\gamma - 1), \quad (2.11)$$

in terms of the renormalized, scale-independent low energy constant \bar{k}_γ .

^{#4}Here, we have already set $Q_L = Q_R = Q$ since we are not concerned with the construction of the effective Lagrangian.

3 Pion form factors

The pion vertex functions with one external vector or scalar source are parametrized in terms of the vector and scalar form factor of the pion, respectively. The vector form factor is experimentally accessible in electron scattering off pions or electron-positron annihilation into a pair of pions. Due to the quantum numbers, the first non-Goldstone meson, the $\rho(770)$, features prominently in this channel and limits the range of applicability of CHPT. However, even at much lower energies, the tail of the ρ is visible, it saturates the LEC \bar{l}_6 and thus largely determines the pion charge radius, as discussed below. The scalar form factor can only be inferred indirectly due to the absence of any external scalar isoscalar source. It plays a central role in the discussion of low energy theorems since the scalar radius is intimately related to the change of the pion decay constant when the quark masses are turned on, as pointed out in ref. [1]. We now turn to a more detailed discussion of these two form factors.

3.1 Vector form factor

The vector form factor of the pion is defined by

$$\langle \pi^a(p') \pi^b(p) \text{ out} | V_\mu^c | 0 \rangle = i \epsilon^{abc} (p'_\mu - p_\mu) F_\pi^V(s), \quad (3.1)$$

with $s = (p' + p)^2$ and V_μ^c the c -component of the quark isovector vector current, $V_\mu^c = \bar{q} \gamma_\mu (\tau^c/2) q$. Gauge invariance requires $F_\pi^V(0) = 1$. Since the neutral pion is its own antiparticle, the corresponding form factor vanishes identically. At next-to-leading order in the chiral expansion, there is no strong isospin breaking in F_π^V [19]. The low energy expansion of the vector form factor defines the electromagnetic charge radius of the pion,

$$F_\pi^V(s) = 1 + \frac{1}{6} \langle r^2 \rangle_\pi^V s + \mathcal{O}(s^2). \quad (3.2)$$

The one-loop representation of F_π^V has been given in [1], whereas the expansion to two loops was worked out using dispersive methods in [4] and by direct diagrammatic calculation in [5]. Here, we are concerned with the virtual photon effects at next-to-leading order (one-loop), including in particular virtual photon loops.

The pertinent Feynman diagrams for a complete calculation at fourth order with virtual photons are depicted in fig. 1. In the first row, we show the strong one-loop graph together with the irreducible one-photon loop diagrams. The second row contains the reducible photon loop diagrams, below the standard wave function renormalization as well as strong and electromagnetic counterterms are depicted. The graphical representation of the Z -factor is also shown. We give here the Z -factors for the neutral and charged pions (note that Z_{π^0} is needed for the calculation of the scalar form factor in the next paragraph),

$$Z_{\pi^0} = 1 - \frac{\Delta_{\pi^0}}{F^2} + e^2 \left(2(2k_3 + k_4) - \frac{20}{9}(k_2 + k_{10}) \right), \quad (3.3)$$

$$Z_{\pi^\pm} = 1 - \frac{\Delta_{\pi^\pm}}{F^2} + 2e^2 \frac{\Delta_{\pi^\pm}}{M_{\pi^\pm}^2} - 2 \left(\frac{e}{4\pi} \right)^2 \left(1 + 2 \log \frac{m_\gamma}{M_{\pi^\pm}} \right) - \frac{20}{9} e^2 (k_2 + k_{10}), \quad (3.4)$$

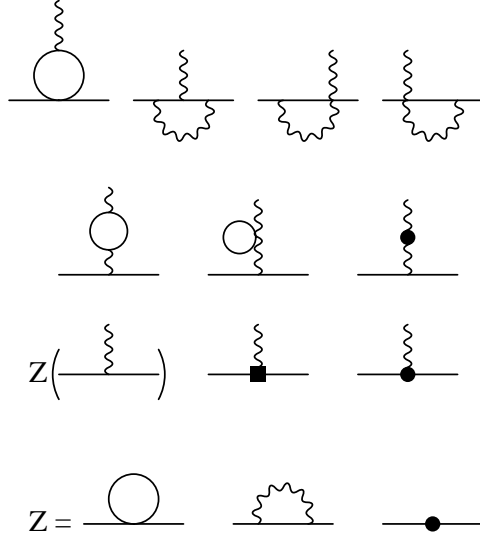


Figure 1: Vector form factor of the pion to one loop. Solid and wiggly lines denote pions and photons, in order. Strong and electromagnetic counterterms are depicted by the filled box and circle, respectively. Diagrams that vanish in dimensional regularization are not shown.

with

$$\Delta_{\pi^a} = 2 M_{\pi^a}^2 \left(L + \frac{1}{(4\pi)^2} \log \frac{M_{\pi^a}}{\lambda} \right). \quad (3.5)$$

Here, L contains the poles in $1/(d-4)$ as $d \rightarrow 4$. Note that the k_i in eqs. (3.3, 3.4) are the non-renormalized LECs of the dimension four counterterms. The photon loop graphs lead to a complication, namely they are not infrared finite. To handle these IR divergences related to the zero photon mass, we introduce a small photon mass m_γ , giving a modified photon propagator

$$D_{\mu\nu}(x) = \int \frac{d^d k}{(2\pi)^d} \frac{-ig_{\mu\nu}}{k^2 - m_\gamma^2 + i\epsilon} e^{-ik \cdot x}. \quad (3.6)$$

Observables are, of course, independent of m_γ , as discussed in section 6. At fourth order, the vector form factor of the pion takes the form:

$$\begin{aligned} F_\pi^V(s) = & 1 + \frac{1}{(4\pi F)^2} \frac{1}{6} \left\{ \left(\bar{l}_6 - \frac{1}{3} \right) s + (4M_{\pi^\pm}^2 - s) K_\pm(s) \right\} \\ & + \left(\frac{e}{4\pi} \right)^2 \left\{ \frac{1}{3} \frac{28M_{\pi^\pm}^2 - 13s}{4M_{\pi^\pm}^2 - s} K_\pm(s) - \frac{4s}{4M_{\pi^\pm}^2 - s} - \frac{4}{3} \left(\frac{M_{\pi^\pm}^2}{s} K_\pm(s) + \frac{1}{6} \right) \right. \\ & \left. + \frac{s - 2M_{\pi^\pm}^2}{M_{\pi^\pm}^2} G(s) + 4 \left(\frac{s - 2M_{\pi^\pm}^2}{s\sigma} \log \frac{\sigma + 1}{\sigma - 1} - 1 \right) \log \frac{m_\gamma}{M_{\pi^\pm}} \right\}, \quad (3.7) \end{aligned}$$

with

$$\sigma = \sqrt{1 - \frac{4M_{\pi^\pm}^2}{s}} \quad (3.8)$$

and

$$K_a(s) = \int_0^1 dx \log\left(1 - x(1-x)\frac{s}{M_a^2}\right), \quad a = \{0, \pm\}, \quad (3.9)$$

$$G(s) = \int_0^1 dx \frac{\log\left(1 - x(1-x)\frac{s}{M_{\pi^\pm}^2}\right)}{1 - x(1-x)\frac{s}{M_{\pi^\pm}^2}}. \quad (3.10)$$

We note that the irreducible photon loop graphs are singular at $s = 4M_{\pi^\pm}^2$ whereas the reducible photon loops are smoothly varying with energy. A representation of $G(s)$ in terms of dilog–functions is given in ref. [10] (since $G(s)$ is related to the IR–finite part of their loop function $G_{+-\gamma}(s)$). The non–renormalization theorem of the electric charge is fulfilled since all the various contributions are of $\mathcal{O}(s)$. This is easily verified using

$$K_a(s) = -\frac{s}{6M_{\pi^a}^2} + \mathcal{O}(s^2), \quad G(s) = -\frac{s}{6M_{\pi^\pm}^2} + \mathcal{O}(s^2). \quad (3.11)$$

In particular, the electromagnetic counterterms from the fourth order Lagrangian, which are momentum–independent, cancel exactly with the corresponding counterterms in the Z –factor, compare fig. 1. Concerning the strong contribution, it is well–known that the counterterm $\sim \bar{l}_6$ dominates the pion charge radius. This LEC is entirely saturated by the ρ –meson, which means that even in the theory of pions only, this resonance plays a visible role.

3.2 Scalar form factor

The scalar form factor of the pion is defined by

$$\langle \pi^a(p') \pi^b(p) \text{ out} | m_u \bar{u}u + m_d \bar{d}d | 0 \rangle = \delta^{ab} \tilde{\Gamma}_\pi(s). \quad (3.12)$$

In order to display the momentum dependence, one introduces the normalized scalar form factor $\Gamma_\pi(s) = \tilde{\Gamma}_\pi(s)/\tilde{\Gamma}_\pi(0)$ so that $\Gamma_\pi(0) = 1$. The low energy expansion of the normalized scalar form factor defines the scalar radius of the pion,

$$\Gamma_\pi(s) = 1 + \frac{1}{6} \langle r^2 \rangle_\pi^S s + \mathcal{O}(s^2). \quad (3.13)$$

Note that while the electromagnetic radius is directly measurable in electron scattering, the absence of scalar–isoscalar external sources allows only for an indirect determination of the scalar radius by e.g. a dispersive analysis of elastic $\pi\pi$ scattering [21]. At $s = 0$, the scalar form factor is proportional to the pion expectation value of the QCD quark mass term

$$\begin{aligned} \mathcal{H}_{\text{QCD}} = m_u \bar{u}u + m_d \bar{d}d &= \frac{1}{2}(m_u + m_d)(\bar{u}u + \bar{d}d) + \frac{1}{2}(m_u - m_d)(\bar{u}u - \bar{d}d) \\ &= \hat{m}(\bar{u}u + \bar{d}d) + \tilde{m}(\bar{u}u - \bar{d}d), \end{aligned} \quad (3.14)$$

in terms of the isoscalar and isovector components. Therefore one can apply the Feynman–Hellman theorem [28, 29] separately to the isoscalar term,

$$\frac{\partial M_\pi^2}{\partial \hat{m}} = \langle \pi | \bar{q}q | \pi \rangle , \quad (3.15)$$

and similarly to the isovector one,

$$\frac{\partial M_\pi^2}{\partial \tilde{m}} = \langle \pi | \bar{q}\tau^3 q | \pi \rangle . \quad (3.16)$$

In the case of virtual photons, the arguments leading to eqs. (3.15, 3.16) are not altered. These equations thus serve as a powerful check on our calculations. The one–loop representation of $\tilde{\Gamma}_\pi$ has been given in [1], whereas the expansion to two loops was worked out using dispersive methods in [4] and by direct diagrammatic calculation in [5]. We are concerned with the virtual photon effects at next–to–leading order. To the order we are working, strong isospin violation only occurs in $\tilde{\Gamma}_\pi(0)$.

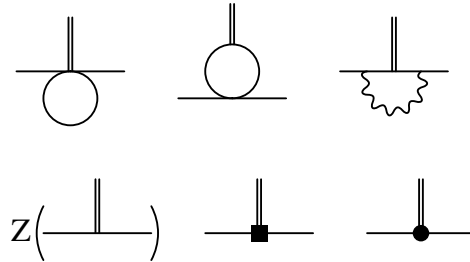


Figure 2: Scalar form factor of the pion to one loop. The double line denotes the coupling to the scalar–isoscalar source. For further notations, see fig. 1.

The pertinent tree level and one–loop Feynman diagrams needed to calculate the scalar form factor at $\mathcal{O}(q^4)$ are shown in fig. 2. The scalar form factor for the charged pions is given by

$$\begin{aligned} \Gamma_{\pi^\pm}(s) = & 1 + \frac{1}{(4\pi F)^2} \left\{ s \left(\bar{l}_4 - 1 - \log \frac{M_{\pi^\pm}}{M_{\pi^0}} \right) + \frac{1}{2} (M_{\pi^0}^2 - s) K_0(s) - \frac{s}{2} K_\pm(s) \right\} \\ & + \left(\frac{e}{4\pi} \right)^2 \left\{ (1 - 4Z) K_\pm(s) + \frac{s - 2M_{\pi^\pm}^2}{M_{\pi^\pm}^2} G(s) \right. \\ & \left. + 4 \left(\frac{s - 2M_{\pi^\pm}^2}{s\sigma} \log \frac{\sigma + 1}{\sigma - 1} - 1 \right) \log \frac{m_\gamma}{M_{\pi^\pm}} \right\} , \end{aligned} \quad (3.17)$$

$$\begin{aligned} \tilde{\Gamma}_{\pi^\pm}(0) = & M_{\pi^\pm}^2 + \frac{M_{\pi^0}^4}{(4\pi F)^2} \frac{1}{2} (1 - \bar{l}_3) - \left(\frac{e}{4\pi} \right)^2 M_{\pi^0}^2 (3 + 4Z) \\ & - 2Ze^2 F^2 \left\{ 1 + \left(\frac{e}{4\pi} \right)^2 \left[4 - (6 + 8Z) \log \frac{M_{\pi^\pm}}{M_{\pi^0}} + \frac{\bar{k}'_\pm}{Z} \right] \right\} , \end{aligned} \quad (3.18)$$

and similarly for the scalar form factor of the neutral pions

$$\Gamma_{\pi^0}(s) = 1 + \frac{1}{(4\pi F)^2} \left\{ s \left(\bar{l}_4 - 1 - 2 \log \frac{M_{\pi^\pm}}{M_{\pi^0}} \right) + (M_{\pi^0}^2 - s) K_\pm(s) - \frac{M_{\pi^0}^2}{2} K_0(s) \right\}, \quad (3.19)$$

$$\tilde{\Gamma}_{\pi^0}(0) = M_{\pi^0}^2 \left\{ 1 + \frac{M_{\pi^0}^2}{(4\pi F)^2} \left(\frac{1}{2}(1 - \bar{l}_3) - 2\bar{l}_7 \delta^2 + 2 \log \frac{M_{\pi^\pm}}{M_{\pi^0}} \right) \right\}, \quad (3.20)$$

with

$$\bar{k}'_\pm = \frac{5}{6} (1 + 2Z + 8Z^2) \bar{k}_1 - \frac{20}{9} Z^2 \bar{k}_2 - \frac{1}{6} (5 + Z + 4Z^2) \bar{k}_9 + \frac{1}{18} (27 + 4Z) Z \bar{k}_{10} \quad (3.21)$$

$$\delta = \frac{m_u - m_d}{m_u + m_d} \approx -0.3, \quad (3.22)$$

and the loop functions $K_a(s)$, $G(s)$ as given in the preceding paragraph. The light quark mass difference only appears in the normalization of the scalar form factor. This is related to the fact that isospin breaking only appears at next-to-leading order, see the last term in eq. (2.4). This operator only has non-vanishing matrix-elements with two neutral pions (similar to the operators c_5 and f_2 which appear in neutral pion scattering off nucleons [16, 18]). To arrive at the formulae for $\tilde{\Gamma}_{\pi^0, \pi^\pm}$, we have made use of the electromagnetic renormalization of the pion masses as given in refs. [9, 10].

4 Effective Lagrangian coupled to gravity

The energy-momentum tensor for chiral effective theories has been studied in ref. [20]. This extended Lagrangian can be constructed by including the metric tensor as an external source which couples to the energy-momentum tensor. At next-to-leading order, one has three new terms (plus additional terms without pions, needed for the renormalization). The energy-momentum tensor plays a role in the pionic decay channels of a hypothetical light Higgs particle via the matrix element $\langle \pi\pi | \Theta_\mu^\mu | 0 \rangle$. We will later use this process to perform the IR regularization of the scalar pion form factor. Here, we briefly collect the pertinent results from ref. [20], adapted to our notation. In addition, we also include virtual photons.

We work in $SU(2)$ and rewrite the terms given in ref. [20] in terms of LECs $l_{11,12,13}$ (note that we keep the numbering as in [20]). The pertinent strong Lagrangian coupled to gravity reads (terms just needed for renormalization are not shown)^{#5}

$$\mathcal{L}^{(4,\text{str},\text{R})} = l_{11} R \langle D_\mu U D^\mu U^\dagger \rangle + l_{12} R^{\mu\nu} \langle D_\mu U D_\nu U^\dagger \rangle + l_{13} R \langle \chi U^\dagger + U \chi^\dagger \rangle, \quad (4.1)$$

where $R_{\mu\nu}$ and R are the Ricci tensor and curvature scalar, respectively,

$$R_{\mu\nu} = R_{\mu\lambda\nu}^\lambda, \quad R = R_\mu^\mu, \quad (4.2)$$

^{#5}At leading order one has no new terms. One simply raises and lowers the Lorentz indices of the non-linear σ -model with the metric tensor $g_{\mu\nu}$.

derived from the curvature tensor and the Christoffel symbols,

$$R_{\sigma\mu\nu}^{\lambda} = \partial_{\mu}\Gamma_{\nu\sigma}^{\lambda} - \partial_{\nu}\Gamma_{\mu\sigma}^{\lambda} + \Gamma_{\mu\alpha}^{\lambda}\Gamma_{\nu\sigma}^{\alpha} - \Gamma_{\nu\alpha}^{\lambda}\Gamma_{\mu\sigma}^{\alpha} , \quad (4.3)$$

$$\Gamma_{\mu\nu}^{\rho} = \frac{1}{2}g^{\rho\sigma}(\partial_{\mu}g_{\nu\sigma} + \partial_{\nu}g_{\mu\sigma} - \partial_{\sigma}g_{\mu\nu}) . \quad (4.4)$$

From these formulae it becomes obvious why R and $R_{\mu\nu}$ count as $\mathcal{O}(q^2)$. For the case of $SU(2)$, the β -functions for l_{11} and l_{13} are

$$\beta_{11} = \frac{1}{6} , \quad \beta_{13} = \frac{1}{8} . \quad (4.5)$$

Note that the coupling l_{12} is not renormalized. For an estimate of the LECs and a more detailed discussion, see ref. [20]. As before, we introduce scale-independent LECs $\bar{l}_{11,12,13}$ as described in sect. 2. As numerical values, we use

$$\bar{l}_{11} = 8.7 , \quad \bar{l}_{12} = -0.4 , \quad \bar{l}_{13} = 9.4 . \quad (4.6)$$

These values have been obtained from the ones given in ref. [20] by running them down to $\lambda = M_{\pi^0}$ using the $SU(3)$ β -functions and converting the obtained values for the renormalized, scale-dependent LECs into the scale-independent ones according to eq. (2.5).

We are interested in the virtual photon corrections to the pionic matrix elements of the energy-momentum tensor. There is exactly one novel electromagnetic counterterm at fourth order,

$$\mathcal{L}^{(4,\text{em},R)} = k_{15} F^2 R \langle QUQU^{\dagger} \rangle . \quad (4.7)$$

Performing standard renormalization, the β -function related to the LEC k_{15} is

$$\beta_{15} = \frac{1}{2} + \frac{2}{3} Z . \quad (4.8)$$

It is obvious from the power counting that there is only one such term. The electric charge has to come in squared, and since R is of order q^2 , we cannot have derivatives on the pion fields or quark mass insertions.

5 Pion form factors of the energy-momentum tensor

Consider now matrix elements of the energy-momentum tensor in one-particle states like e.g. the pion. The general form of such matrix elements follows from Lorentz invariance and four-momentum conservation [20],

$$\langle \pi^a(p') | \Theta_{\mu\nu} | \pi^b(p) \rangle = \delta^{ab} \left[\frac{1}{2}(s g_{\mu\nu} - q_{\mu}q_{\nu}) \Theta_1(s) + \frac{1}{2}P_{\mu}P_{\nu} \Theta_2(s) \right] , \quad (5.1)$$

with $P_{\mu} = p'_{\mu} + p_{\mu}$, $q_{\mu} = p'_{\mu} - p_{\mu}$, and $s = q^2$. The two form factors reflect the fact that the energy-momentum tensor contains a scalar and a tensor part. In what follows, we are mostly

interested in the matrix element of the trace of the energy–momentum tensor, Θ_μ^μ , which is a scalar. The corresponding matrix element takes the form (neglecting isospin indices)

$$\langle \pi | \Theta_\mu^\mu | \pi \rangle \equiv \Theta_\pi(s) = \frac{3}{2}s \Theta_1(s) + \frac{1}{2}(4M_\pi^2 - s) \Theta_2(s) . \quad (5.2)$$

Because Θ_{00} is the Hamiltonian density, we require the normalization $\Theta_2(0) = 1$.

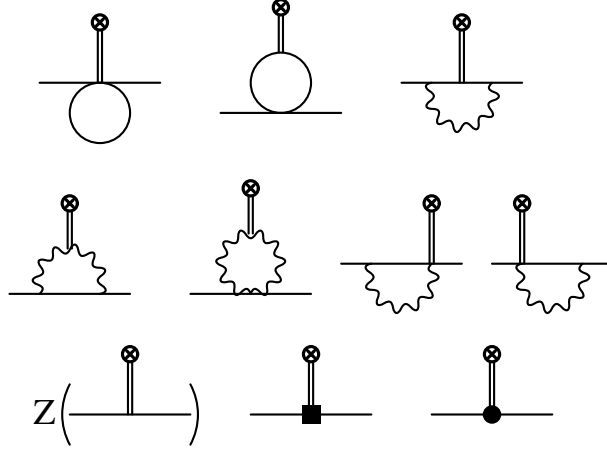


Figure 3: Pion form factors of the energy–momentum tensor to one loop. The double line with the circle-cross denotes the coupling to the energy–momentum tensor. For further notations, see fig. 1.

The pertinent Feynman diagrams needed to evaluate the form factors of the energy–momentum tensor at next–to–leading order (including virtual photons) in one–pion states are shown in fig. 3. At tree level, one simply has $\Theta_1(s) = \Theta_2(s) = 1$. The full one–loop result for the charged pions reads

$$\begin{aligned} \frac{\Theta_1^{\pi^\pm}(s)}{\Theta_1^{\pi^\pm}(0)^{\text{fin}}} &= 1 - \frac{1}{(4\pi F)^2} \left\{ \frac{8}{9}s - 2s \log \frac{M_{\pi^\pm}}{M_{\pi^0}} + \frac{1}{3}(s + M_{\pi^0}^2) K_0(s) + \frac{1}{3}(s + 2M_{\pi^\pm}^2) K_\pm(s) \right. \\ &\quad \left. - \frac{2}{3}M_{\pi^0}^2 \left(\frac{M_{\pi^0}^2}{s} K_0(s) + \frac{1}{6} \right) - 2s \left(\frac{1}{3}\bar{l}_{11} + \bar{l}_{12} \right) \right\} \\ &\quad + \left(\frac{e}{4\pi} \right)^2 \left\{ \frac{8}{3}(1 + Z)K_\pm(s) + \frac{8}{3}(2Z - 1) \left(\frac{M_{\pi^\pm}^2}{s} K_\pm(s) + \frac{1}{6} \right) \right. \\ &\quad \left. + \frac{s - 2M_{\pi^\pm}^2}{M_{\pi^\pm}^2} G(s) + 2M_{\pi^\pm}^2 (H(s) - 2H_1(s)) \right. \\ &\quad \left. - \frac{2}{3} \left(\log \frac{s}{M_{\pi^\pm}^2} - i\pi \right) + 4 \left(\frac{s - 2M_{\pi^\pm}^2}{s\sigma} \log \frac{\sigma + 1}{\sigma - 1} - 1 \right) \log \frac{m_\gamma}{M_{\pi^\pm}} \right\} , \quad (5.3) \\ \Theta_1^{\pi^\pm}(0)^{\text{fin}} &= 1 + \frac{M_{\pi^0}^2}{(4\pi F)^2} \left\{ \frac{1}{3} - \frac{4}{3} \log \frac{M_{\pi^\pm}}{M_{\pi^0}} + \bar{l}_{13} - \frac{4}{3}\bar{l}_{11} \right\} \end{aligned}$$

$$+ \left(\frac{e}{4\pi} \right)^2 \left\{ \frac{8}{9} (2 + 3Z) + \left(2 + \frac{8}{3} Z \right) \left(\bar{k}_{15} + 2 \log \frac{M_{\pi^\pm}}{M_{\pi^0}} \right) \right\}, \quad (5.4)$$

$$\begin{aligned} \Theta_2^{\pi^\pm}(s) &= 1 - \frac{2s}{(4\pi F)^2} \bar{l}_{12} \\ &+ \left(\frac{e}{4\pi} \right)^2 \left\{ \frac{4s}{s - 4M_{\pi^\pm}^2} + 6 \frac{s - 2M_{\pi^\pm}^2}{s - 4M_{\pi^\pm}^2} K_\pm(s) + \frac{s - 2M_{\pi^\pm}^2}{M_{\pi^\pm}^2} G(s) \right. \\ &\quad + \left(2M_{\pi^\pm}^2 (H(s) - 2H_1(s)) - \frac{2}{3} \left(\log \frac{s}{M_{\pi^\pm}^2} - i\pi \right) \right) \frac{3s}{s - 4M_{\pi^\pm}^2} \\ &\quad \left. + 4 \left(\frac{s - 2M_{\pi^\pm}^2}{s\sigma} \log \frac{\sigma + 1}{\sigma - 1} - 1 \right) \log \frac{m_\gamma}{M_{\pi^\pm}} \right\}, \quad (5.5) \end{aligned}$$

and similarly for the neutral pions we find

$$\begin{aligned} \frac{\Theta_1^{\pi^0}(s)}{\Theta_1^{\pi^0}(0)} &= 1 - \frac{1}{(4\pi F)^2} \left\{ \frac{8}{9} s + \frac{4}{3} s \log \frac{M_{\pi^\pm}}{M_{\pi^0}} + \frac{2}{3} (s + 2M_{\pi^\pm}^2 - M_{\pi^0}^2) K_\pm(s) + \frac{1}{3} M_{\pi^0}^2 K_0(s) \right. \\ &\quad \left. - \frac{4}{3} M_{\pi^0}^2 \left(\frac{M_{\pi^\pm}^2}{s} K_\pm(s) + \frac{1}{6} \right) + \frac{2}{3} M_{\pi^0}^2 \left(\frac{M_{\pi^0}^2}{s} K_0(s) + \frac{1}{6} \right) - 2s \left(\frac{1}{3} \bar{l}_{11} + \bar{l}_{12} \right) \right\}, \quad (5.6) \end{aligned}$$

$$\Theta_1^{\pi^0}(0) = 1 + \frac{M_{\pi^0}^2}{(4\pi F)^2} \left\{ \frac{1}{3} + \frac{4}{3} \log \frac{M_{\pi^\pm}}{M_{\pi^0}} + \bar{l}_{13} - \frac{4}{3} \bar{l}_{11} \right\}, \quad (5.7)$$

$$\Theta_2^{\pi^0}(s) = 1 - \frac{2s}{(4\pi F)^2} \bar{l}_{12}, \quad (5.8)$$

in terms of the loop functions $K_{0,\pm}(s)$, $G(s)$ defined in eqs. (3.9, 3.10) and

$$H(s) = \frac{1}{s\sigma} \left\{ \left(\frac{1}{2} \log \frac{s}{M_{\pi^\pm}^2} - i\pi \right) \log \frac{1 + \sigma}{1 - \sigma} - \int_{\tau_-}^{\tau_+} dt \frac{\log t}{1 - t} \right\}, \quad (5.9)$$

$$H_1(s) = \frac{1}{\sigma^2} \left\{ \frac{1}{2} H(s) - \frac{1}{s} \left(\log \frac{s}{M_{\pi^\pm}^2} - i\pi \right) \right\}, \quad (5.10)$$

with

$$\tau_\pm = \frac{1 \pm \sigma - 2M_{\pi^\pm}^2/s}{1 \pm \sigma}. \quad (5.11)$$

The following remarks are in order. First, in the isospin limit ($m_u = m_d$, $e^2 = 0$) we recover the results of ref. [20]. The normalization of $\Theta_2(0)$ is not affected by the photon loops, in particular not by the IR divergent terms. We also note that for the charged pions, Θ_1 diverges logarithmically at $s = 0$. We have therefore only given the finite part of $\Theta_1^{\pi^\pm}(0)$, denoted by the superscript “fin”. This divergence is due to the photon tadpole and self-energy graphs with coupling of the energy-momentum tensor to the photon line. Such diagrams are not present in the case of the scalar pion form factor simply because a scalar-isoscalar source has no coupling to virtual photons only. We remark that after mass renormalization, no counterterms from $\mathcal{L}^{(4, \text{str})}$ and $\mathcal{L}^{(4, \text{em})}$ contribute to $\Theta_{1,2}^{\pi^a}$. Finally, we note that the new loop functions $H(s)$ and $H_1(s)$ cancel in the matrix elements of the trace of the energy-momentum tensor as defined in eq. (5.2). Consequently, these matrix elements are well behaved at $s = 0$.

We can now combine the results collected in eqs. (5.3–5.8) to work out the pionic form factors of the trace of the energy–momentum tensor. For the charged pions this leads to

$$\begin{aligned}
\Theta_{\pi^\pm}(s) &= 2M_{\pi^\pm}^2 + s \\
&+ \frac{1}{(4\pi F)^2} \left\{ \frac{2}{3}(M_{\pi^0}^2 - 2s)s + s(3s - 2M_{\pi^0}^2) \log \frac{M_{\pi^\pm}}{M_{\pi^0}} - \frac{1}{2}(s - M_{\pi^0}^2)(s + 2M_{\pi^0}^2) K_0(s) \right. \\
&\quad \left. - \frac{1}{2}s(s + 2M_{\pi^\pm}^2) K_\pm(s) + s(s - 2M_{\pi^0}^2) \bar{l}_{11} + 4s(s - M_{\pi^0}^2) \bar{l}_{12} + \frac{3}{2}sM_{\pi^0}^2 \bar{l}_{13} \right\} \\
&+ \left(\frac{e}{4\pi} \right)^2 \left\{ (2M_{\pi^\pm}^2 + s)(1 + 4Z) K_\pm(s) \right. \\
&\quad + (2M_{\pi^\pm}^2 + s) \frac{s - 2M_{\pi^\pm}^2}{M_{\pi^\pm}^2} G(s) + (3 + 4Z)s \left(\bar{k}_{15} + 2 \log \frac{M_{\pi^\pm}}{M_{\pi^0}} \right) \\
&\quad \left. + 4(2M_{\pi^\pm}^2 + s) \left(\frac{s - 2M_{\pi^\pm}^2}{s\sigma} \log \frac{\sigma + 1}{\sigma - 1} - 1 \right) \log \frac{m_\gamma}{M_{\pi^\pm}} \right\}, \tag{5.12}
\end{aligned}$$

and similarly for the neutral pions

$$\begin{aligned}
\Theta_{\pi^0}(s) &= 2M_{\pi^0}^2 + s \\
&+ \frac{1}{(4\pi F)^2} \left\{ \frac{2}{3}(M_{\pi^0}^2 - 2s)s - 2s(s - M_{\pi^0}^2) \log \frac{M_{\pi^\pm}}{M_{\pi^0}} - \frac{1}{2}M_{\pi^0}^2(s + 2M_{\pi^0}^2) K_0(s) \right. \\
&\quad \left. - (s - M_{\pi^0}^2)(s + 2M_{\pi^0}^2) K_\pm(s) + s(s - 2M_{\pi^0}^2) \bar{l}_{11} + 4s(s - M_{\pi^0}^2) \bar{l}_{12} + \frac{3}{2}sM_{\pi^0}^2 \bar{l}_{13} \right\}. \tag{5.13}
\end{aligned}$$

One process in which these form factors play a role is the decay of a light Higgs boson into a pion pair. The corresponding matrix element takes the form [21]

$$\langle \pi^i(p) \pi^k(p') | \mathcal{L}_{\text{eff}} | H \rangle = -\frac{1}{v} \mathcal{G}(s) \delta^{ik}, \quad \mathcal{G}(s) = \frac{2}{9} \Theta_\pi(s) + \frac{7}{9} (\tilde{\Gamma}_\pi(s) + S_\pi(s)), \tag{5.14}$$

where H denotes the Higgs field and the form factor S_π is related to the expectation value of the strangeness operator $m_s \bar{s}s$ in the pion. In what follows, we will neglect this form factor. Also, v is the scale of electroweak symmetry breaking, $v^{-2} = \sqrt{2}G_F \simeq (250 \text{ GeV})^{-2}$ (with G_F the Fermi constant). The width of the Higgs decaying into a pair of charged pions is then given by

$$\Gamma(H \rightarrow \pi^+ \pi^-) = \frac{\sqrt{2}G_F}{16\pi m_H} \sqrt{1 - \frac{4M_{\pi^\pm}^2}{m_H^2}} |\mathcal{G}(m_H^2)|^2, \tag{5.15}$$

with m_H the Higgs mass. For more details, we refer to ref. [21].

6 Infrared regularization

So far we have dealt with the IR divergences by introducing a small photon mass m_γ . We are now going to cure this by considering processes with additional soft photon radiation from

the final–state pions with photon energies below a given detector resolution ΔE . Before discussing the details for the various form factors, we have to address the power counting. In fact, for the treatment of IR divergences, only the counting in e (or, equivalently, in the fine structure constant α) is of relevance. Since we consider one–photon loop diagrams, these scale as e^2 . Any radiation of a single soft photon carries a factor of e in a given amplitude, so that, for a pertinent cross section (which is the square of such an amplitude), we get contributions of order e^2 . Radiation of multiple soft photons is therefore related to higher order photon loop diagrams. The procedure we have to follow is standard, for a textbook treatment we refer e.g. to refs. [30, 31]. Consequently, we do not concern ourselves here with initial state radiation.

6.1 Vector form factor

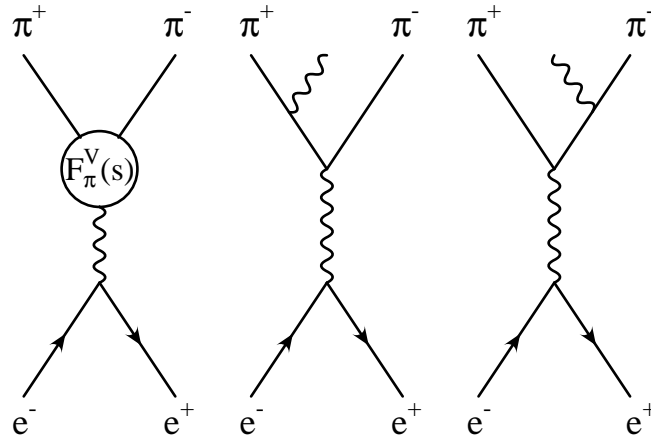


Figure 4: IR regularization of the vector form factor to one loop. The photon radiated from the charged pion lines is soft.

Consider now the vector form factor. As shown in fig. 4, it can be measured e.g. in electron–positron annihilation. The corresponding tree graphs with soft photon radiation are also depicted in that figure. We evaluate the square of the vector form factor. After the IR regularization procedure, it takes the form

$$\begin{aligned}
|F_\pi^V(s)|^2 &= 1 + \frac{1}{(4\pi F)^2} \frac{1}{3} \left\{ \left(\bar{l}_6 - \frac{1}{3} \right) s + (4M_{\pi^\pm}^2 - s) K_\pm(s) \right\} \\
&+ 2 \left(\frac{e}{4\pi} \right)^2 \left\{ \frac{1}{3} \frac{28M_{\pi^\pm}^2 - 13s}{4M_{\pi^\pm}^2 - s} K_\pm(s) - \frac{4s}{4M_{\pi^\pm}^2 - s} - \frac{4}{3} \left(\frac{M_{\pi^\pm}^2}{s} K_\pm(s) + \frac{1}{6} \right) \right. \\
&\left. + \frac{s - 2M_{\pi^\pm}^2}{M_{\pi^\pm}^2} G(s) + 4 \left(\frac{s - 2M_{\pi^\pm}^2}{s\sigma} \log \frac{\sigma + 1}{\sigma - 1} - 1 \right) \log \frac{\Delta E}{M_{\pi^\pm}} + R_V(s, \Delta E) \right\} \quad (6.1)
\end{aligned}$$

with the resolution function $R_V(s, \Delta E)$

$$\begin{aligned}
R_V(s, \Delta E) &= \frac{s - m_e^2}{s + 2m_e^2} \frac{16}{s \sigma^3} \int_0^{\Delta E} dl l \sqrt{\left(1 - \frac{2l}{\sqrt{s}}\right) \left(1 - \frac{4M_{\pi^\pm}^2}{s} - \frac{2l}{\sqrt{s}}\right)} \\
&- 12 \frac{M_{\pi^\pm}^2}{s + 2m_e^2} \frac{1}{s \sigma^3} \int_0^{\Delta E} dl l \sigma(l) - 4 \frac{1}{\sqrt{s} \sigma} \int_0^{\Delta E} dl \log\left(\frac{1 + \sigma(l)}{1 - \sigma(l)}\right) \\
&- \frac{s - 4m_e^2}{s + 2m_e^2} \frac{s - 2M_{\pi^\pm}^2}{s^2 \sigma^3} \int_0^{\Delta E} dl l \log\left(\frac{1 + \sigma(l)}{1 - \sigma(l)}\right) \\
&- \frac{4M_{\pi^\pm}^2}{s \sigma} \int_0^{\Delta E} \frac{dl}{l} \left(\frac{\sigma(l)}{1 - \sigma^2(l)} - \frac{s \sigma}{4M_{\pi^\pm}^2}\right) \\
&+ \frac{s - 2M_{\pi^\pm}^2}{s \sigma} \int_0^{\Delta E} \frac{dl}{l} \log\left(\frac{1 + \sigma(l)}{1 - \sigma(l)} \frac{1 - \sigma}{1 + \sigma}\right), \tag{6.2}
\end{aligned}$$

where

$$\sigma(l) = \sqrt{\frac{s - 4M_{\pi^\pm}^2 - 2\sqrt{s}l}{s - 2\sqrt{s}l}}, \tag{6.3}$$

$\sigma(0) = \sigma$ as defined in eq. (3.8), and m_e is the electron mass. ΔE is the detector resolution which should be supplied by the experimenters. Typically, $\Delta E = 10 \dots 20$ MeV. The resulting expression is obviously IR finite. For later discussion, we call the term $\sim \log(\Delta E/M_{\pi^\pm})$ the IR finite contribution and the term proportional to the resolution function the finite bremsstrahlung contribution. Finally, we remark that if one chooses a different process to perform the IR regularization, the resolution function would be different.

6.2 Higgs decay and scalar form factors

We now turn to the IR regularization of the scalar form factors. Let us genuinely denote by $S_{\pi^\pm}(s)$ any one of the charged pion scalar form factors $\tilde{\Gamma}_{\pi^\pm}(s)$, $\Theta_{\pi^\pm}(s)$, or any linear combination thereof. To the order we are working, the regularization can be performed by considering a physical process like the decay of a light Higgs H into two pions accompanied by soft photon radiation from the final-state pions. The isospin-conserving part of this process has been studied in great detail in ref. [21], see also ref. [22]. We have used that calculation as a check whenever possible. Of course, the calculation is somewhat academic since such a light Higgs seems to be ruled out by experiment. It is, however, the simplest process which allows us to perform the IR regularization. Alternatively, one could consider processes like $\psi' \rightarrow \psi \pi \pi$. More precisely, we only need to consider the emission of *one* soft photon from any one of the charged pions in the final-state. The method is depicted in fig. 5, which shows the tree graph for the $H \rightarrow \pi \pi$ decay via the corresponding scalar form factor and the two graphs with one soft photon. Denote by $S_{\pi^\pm}^{(0)}(s)$ the leading term in the chiral expansion of any scalar form factor and by $S_{\pi^\pm}^{(2)}(s)$ the next-to-leading order contribution. To one-loop accuracy, the IR-divergent part of the amplitude takes the form

$$S_{\pi^\pm}^{(2, \text{IR-div})}(s) = 4 \left(\frac{e}{4\pi}\right)^2 S_{\pi^\pm}^{(0)}(s) \xi \log \frac{m_\gamma}{M_{\pi^\pm}}, \tag{6.4}$$

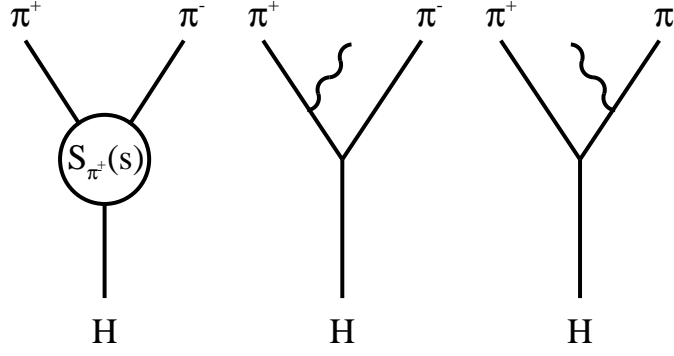


Figure 5: IR regularization of any scalar form factor $S_{\pi^\pm}(s)$ to one loop. The solid line labeled “H” denotes the light Higgs particle. The photon radiated from the charged pion lines is soft.

with

$$\xi = \frac{s - 2M_{\pi^\pm}^2}{s\sigma} \log \frac{\sigma + 1}{\sigma - 1} - 1. \quad (6.5)$$

With that, we can write the square of the form factor as

$$\begin{aligned} |S_{\pi^\pm}(s)|^2 &= |S_{\pi^\pm}^{(0)}(s)|^2 \left\{ 1 + 8 \left(\frac{e}{4\pi} \right)^2 \xi \log \frac{\Delta E}{M_{\pi^\pm}} + \left(\frac{e}{4\pi} \right)^2 R_S(s, \Delta E) \right\} \\ &\quad + 2 \operatorname{Re} S_{\pi^\pm}^{(0)}(s) S_{\pi^\pm}^{(2, \text{fin})}(s) + \mathcal{O}(e^4), \end{aligned} \quad (6.6)$$

with the resolution function $R_S(s, \Delta E)$ given by

$$\begin{aligned} R_S(s, \Delta E) &= -\frac{16}{s\sigma} \left\{ 2M_{\pi^\pm}^2 \int_0^{\Delta E} \frac{dl}{l} \left(\frac{\sigma(l)}{1 - \sigma^2(l)} - \frac{s\sigma}{4M_{\pi^\pm}^2} \right) + \sqrt{s} \int_0^{\Delta E} dl \log \left(\frac{1 + \sigma(l)}{1 - \sigma(l)} \right) \right. \\ &\quad \left. + \left(M_{\pi^\pm}^2 - \frac{s}{2} \right) \int_0^{\Delta E} \frac{dl}{l} \log \left(\frac{1 + \sigma(l)}{1 - \sigma(l)} \frac{1 - \sigma}{1 + \sigma} \right) \right\}, \end{aligned} \quad (6.7)$$

where $\sigma(l)$ has been defined in eq. (6.3) and $\sigma(0) = \sigma$ in eq. (3.8), respectively. Again, the term $\sim \xi$ leads to the IR finite pieces and the term $\sim R_S$ to the finite bremsstrahlung contribution. We refrain from writing down the explicit IR finite expressions for the various scalar form factors since they can be deduced easily from eq. (6.6) and the formulae spelled out in sections 3 and 5.

7 Results and discussion

7.1 Vector form factor and pion charge radius

In fig. 6, we show the vector form factor in the time-like region. We remark that the electromagnetic corrections from the reducible photon loops and from the bremsstrahlung

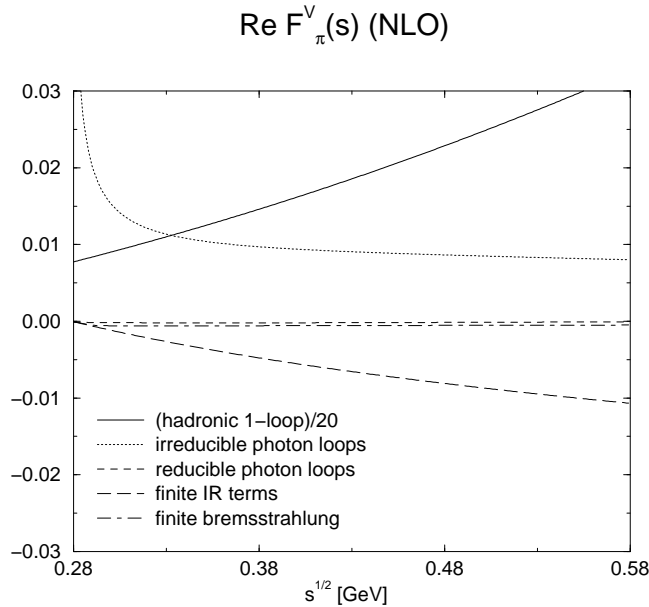


Figure 6: Vector form factor in the time-like region. The various virtual photon contributions are shown in comparison with the strong fourth order contribution. The latter is divided by a factor of 20.

are very small, the latter contribution being so tiny that it will be discarded in what follows. A bit above threshold, the finite IR terms are of similar size as the irreducible photon loop contribution. For comparison, we have also shown the strong fourth order contribution divided by a factor of 20. We conclude that the electromagnetic corrections are of the expected size of about one percent, except for the divergence of the photon loop graphs at $s = 4M_{\pi^\pm}^2$. In the space-like region, shown in fig. 7, the electromagnetic effects from the finite IR graphs are somewhat more pronounced, the photon loop contribution is small. From this, we can deduce the electromagnetic corrections to the pion charge radius,

$$\langle r^2 \rangle_{\pi, \text{strong}}^V = \frac{1}{(4\pi F)^2} (\bar{l}_6 - 1), \quad (7.1)$$

$$\langle r^2 \rangle_{\pi, \text{photon}}^V = -\left(\frac{e}{4\pi}\right)^2 \frac{31}{5M_{\pi^\pm}^2}, \quad (7.2)$$

$$\langle r^2 \rangle_{\pi, \text{finite IR}}^V = -\left(\frac{e}{4\pi}\right)^2 \frac{8}{M_{\pi^\pm}^2} \log \frac{\Delta E}{M_{\pi^\pm}}. \quad (7.3)$$

The numerical results for these various contributions are

$$\langle r^2 \rangle_{\pi, \text{strong}}^V = 0.442 \text{ fm}^2, \quad \langle r^2 \rangle_{\pi, \text{photon}}^V = -0.007 \text{ fm}^2, \quad \langle r^2 \rangle_{\pi, \text{finite IR}}^V = 0.024 (0.018) \text{ fm}^2, \quad (7.4)$$

for $\Delta E = 10 (20)$ MeV. We use $F = 93$ MeV, $M_{\pi^\pm} = 139.57$ MeV and $\bar{l}_6 = 16.5$. There are two ways of dealing with the resolution dependent IR contribution. First, if one compares the similar process $e^+e^- \rightarrow \mu^+\mu^-$, soft photon radiation to leading order in e^2 gives a

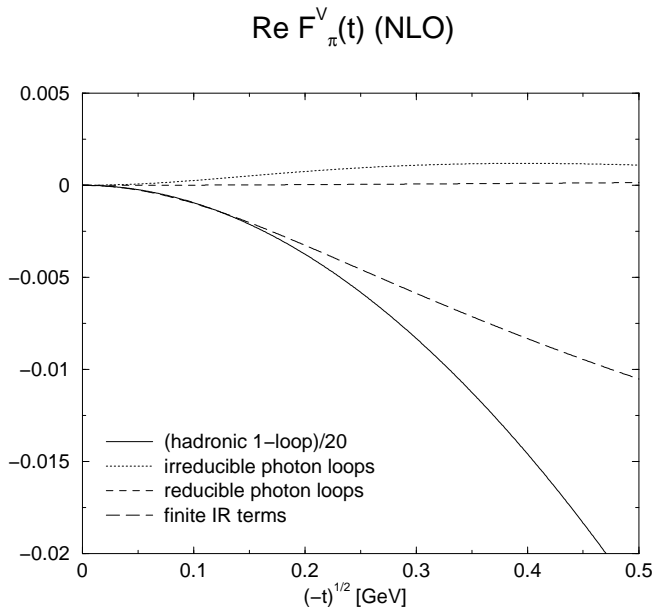


Figure 7: Vector form factor in the space-like region. The various virtual photon contributions are shown in comparison with the strong fourth order contribution. The latter is divided by a factor of 20.

finite IR contribution to the “intrinsic” muon radius, which is believed to be zero. This contribution has the same form as in eq. (7.3) but with the pion mass replaced by the muon mass (see e.g. the explicit calculation in ref. [30]). If one therefore directly compares the processes $e^+e^- \rightarrow \pi^+\pi^-(\gamma)$ and $e^+e^- \rightarrow \mu^+\mu^-(\gamma)$, one is only sensitive to the difference $(1/M_{\pi^\pm}) \log(\Delta E/M_{\pi^\pm}) - (1/M_\mu) \log(\Delta E/M_\mu)$ which reduces the dependence on the detector resolution by almost one order of magnitude. Another way of proceeding is to follow the arguments which have been used in the discussion of $\pi\pi$ scattering [32, 10]. While the cross section of course depends on the detector resolution and so does the scattering length a , $d\sigma/d\Omega = |a|^2$, one can define an electromagnetically corrected scattering length which is independent of ΔE . This is achieved by absorbing the resolution dependent terms into the appropriately redefined phase space. Such a procedure applied here would essentially amount to dropping the term given in eq. (7.3). To summarise, the resolution dependent terms are probably not to be understood as “real” isospin violation effects in the reaction $e^+e^- \rightarrow \pi^+\pi^-$, but rather as part of the radiative process $e^+e^- \rightarrow \pi^+\pi^-\gamma$, and therefore should not be regarded as intrinsic electromagnetic corrections to the form factor.

We should explicitly compare these numbers to the two-loop corrections for the vector form factor calculated in ref. [5]. Depending on the set of parameters they use, they find corrections at $\mathcal{O}(q^6)$ which numerically amount to

$$\langle r^2 \rangle_{\pi, 2\text{-loop}}^V = 0.017 \dots 0.022 \text{ fm}^2 . \quad (7.5)$$

This is larger than the “intrinsic” virtual photon contribution found above by about a factor of 3, and thus is similar to the findings in the pion-pion scattering case, see refs. [9, 10].

In refs. [4, 5], also the quadratic term in the Taylor expansion of $F_\pi^V(s)$ according to

$$F_\pi^V(s) = 1 + \frac{1}{6} \langle r^2 \rangle_\pi^V s + c_\pi^V s^2 + \mathcal{O}(s^3) \quad (7.6)$$

was considered. Counterterms to fit experimental values of c_π^V exactly only appear at $\mathcal{O}(q^6)$, and indeed the finding in [4, 5] is that the $\mathcal{O}(q^4)$ calculation is completely insufficient to describe c_π^V , with the final value dominated by an $\mathcal{O}(q^6)$ counterterm. Here, we might either check whether this large $\mathcal{O}(q^6)$ contribution can be reduced when taking into account the electromagnetic corrections, or we can give credit to the two-loop analysis in case these again turn out to be very small. The contributions found from expanding eq. (3.7) are

$$c_{\pi,\text{strong}}^V = \frac{1}{(4\pi F)^2} \frac{1}{60M_{\pi^\pm}^2} = 0.626 \text{ GeV}^{-4}, \quad (7.7)$$

$$c_{\pi,\text{photon}}^V = -\left(\frac{e}{4\pi}\right)^2 \frac{113}{420M_{\pi^\pm}^4} = -0.412 \text{ GeV}^{-4}, \quad (7.8)$$

$$c_{\pi,\text{finiteIR}}^V = -\left(\frac{e}{4\pi}\right)^2 \frac{1}{5M_{\pi^\pm}^4} \log \frac{\Delta E}{M_{\pi^\pm}} = 0.807 (0.595) \text{ GeV}^{-4}, \quad (7.9)$$

for $\Delta E = 10$ (20) MeV, whereas, for comparison, the authors of [5] give a value of

$$c_\pi^V = (3.85 \pm 0.60) \text{ GeV}^{-4}, \quad (7.10)$$

found by a fit of the $\mathcal{O}(q^6)$ CHPT amplitude to the data. We see therefore that the electromagnetic effects on the curvature are of a size comparable to the hadronic one-loop parts, although resolution dependent and independent contributions tend to cancel to some extent for typical values of ΔE . In the analysis of ref. [5], this would lead to a moderate change in their LEC r_{V2}^r .

We conclude that, throughout, the intrinsic virtual photon effects on the pion vector form factor in the low energy region are of the expected size and smaller than the two loop effects calculated in refs. [4, 5]. (Note finally that one particular $SU(3)$ effect (the charged to neutral kaon mass difference in kaon loops) has also been found to be tiny, see ref. [33].)

7.2 Scalar form factor and scalar pion radius

We now turn to the scalar form factor. In contrast to the vector form factor, we have an additional electromagnetic effect, namely the pion mass difference in the hadronic loops (of course, there is also a tiny strong contribution to the pion mass splitting).

Consider the charged pions first. The various virtual photon corrections are shown in fig. 8 in comparison with the strong fourth order contribution scaled down by a factor of 20. Here, the different contributions are somewhat more pronounced as compared to the vector case, but again we observe cancellations between the various effects. Note that the finite

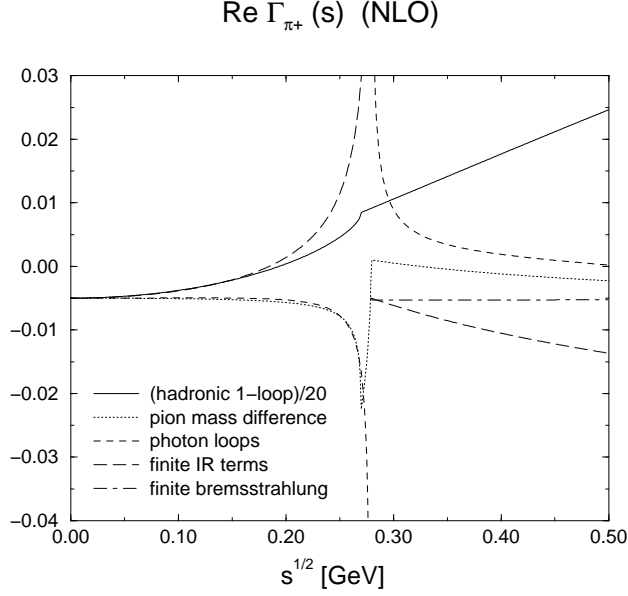


Figure 8: Scalar form factor of the charged pions in the time-like region. The various virtual photon contributions are shown in comparison with the strong fourth order contribution. The latter is divided by a factor of 20.

bremsstrahlung contribution is again very small. The corresponding corrections to the scalar radius of the pion can be worked out easily (we again neglect the tiny bremsstrahlung piece),

$$\langle r^2 \rangle_{\pi^\pm, \text{strong}}^S = \frac{6}{(4\pi F)^2} \left(\bar{l}_4 - \frac{13}{12} \right), \quad (7.11)$$

$$\langle r^2 \rangle_{\pi^\pm, \text{mass}}^S = -\frac{6}{(4\pi F)^2} \log \frac{M_{\pi^\pm}}{M_{\pi^0}} + \left(\frac{e}{4\pi} \right)^2 \frac{4Z}{M_{\pi^\pm}^2}, \quad (7.12)$$

$$\langle r^2 \rangle_{\pi^\pm, \text{photon}}^S = \left(\frac{e}{4\pi} \right)^2 \frac{1}{M_{\pi^\pm}^2}, \quad (7.13)$$

$$\langle r^2 \rangle_{\pi^\pm, \text{finite IR}}^S = -\left(\frac{e}{4\pi} \right)^2 \frac{8}{M_{\pi^\pm}^2} \log \frac{\Delta E}{M_{\pi^\pm}}. \quad (7.14)$$

The novel contribution due to the pion mass difference in the pion loops is denoted by the subscript “mass”. The resolution dependent term is identical to the one obtained for the vector form factor. It can be dealt with in the same manner as described in the preceding paragraph. The corresponding values are

$$\begin{aligned} \langle r^2 \rangle_{\pi^\pm, \text{strong}}^S &= 0.550 \text{ fm}^2, & \langle r^2 \rangle_{\pi^\pm, \text{mass}}^S &= -0.0016 \text{ fm}^2, \\ \langle r^2 \rangle_{\pi^\pm, \text{photon}}^S &= 0.0012 \text{ fm}^2, & \langle r^2 \rangle_{\pi^\pm, \text{finite IR}}^S &= 0.024 (0.018) \text{ fm}^2, \end{aligned} \quad (7.15)$$

for $\Delta E = 10 (20)$ MeV and using $\bar{l}_4 = 4.3$. We note that the small corrections due to the pion mass difference (-0.3%) and the photon loops ($+0.2\%$) nearly cancel each other to

give a tiny effect on the radius. Even the separate contributions are, again, by one order of magnitude smaller than the two-loop corrections [5],

$$\langle r^2 \rangle_{\pi,2\text{-loop}}^S = 0.016 \dots 0.025 \text{ fm}^2 . \quad (7.16)$$

The normalization of the scalar form factor is also of interest. We normalize it here to the mass of the charged pions (although the canonical reference mass is the one of the neutral pion),

$$\tilde{\Gamma}_{\pi^\pm}(0) = M_{\pi^\pm}^2 (1 - 0.065 - 0.012 - 0.004) , \quad (7.17)$$

where the first correction is due to the electromagnetic operator $\sim C$, i.e. the pion mass difference, the second term is the well-known hadronic shift [1] (using $\bar{l}_3 = 2.9$), and the third term comprises the genuine electromagnetic corrections. To arrive at this last number, we have used the dimensional analysis of ref. [10], $|k_i^r(M_\rho)| \leq 1/(4\pi)^2$, which leads to $|\bar{k}'_\pm| \leq 6.3$. Consequently, the shift due to the electromagnetic corrections is about one third of the strong correction to the normalization of the charged pions scalar form factor.

As in the case of the vector form factor, we wish to give credit to the analysis of the quadratic term of the Taylor expansion of the form factors given in refs. [4, 5]. The remarks made about the purpose of such an analysis for the one-loop electromagnetic corrections in the case of $F_\pi^V(s)$ apply equally here. From eq. (3.17) we find

$$c_{\pi^\pm,\text{strong}}^S = \frac{1}{(4\pi F)^2} \frac{19}{120M_{\pi^0}^2} = 6.36 \text{ GeV}^{-4} , \quad (7.18)$$

$$c_{\pi^\pm,\text{mass}}^S = \left(\frac{e}{4\pi}\right)^2 \frac{Z}{M_{\pi^\pm}^2} \left(\frac{1}{15M_{\pi^\pm}^2} - \frac{1}{6M_{\pi^0}^2}\right) = -0.15 \text{ GeV}^{-4} , \quad (7.19)$$

$$c_{\pi^\pm,\text{photon}}^S = -\left(\frac{e}{4\pi}\right)^2 \frac{1}{12M_{\pi^\pm}^4} = -0.13 \text{ GeV}^{-4} , \quad (7.20)$$

$$c_{\pi^\pm,\text{finiteIR}}^S = -\left(\frac{e}{4\pi}\right)^2 \frac{1}{5M_{\pi^\pm}^4} \log \frac{\Delta E}{M_{\pi^\pm}} = 0.81 (0.60) \text{ GeV}^{-4} . \quad (7.21)$$

Note that the difference in the numerical value for the hadronic one-loop contribution as compared to ref. [5] occurs because they employ the charged pion mass whereas, when taking isospin violation into account, the correct reference mass is the neutral pion mass. The value extracted from experimental data is [4, 5]

$$c_\pi^S = (10.6 \pm 0.6) \text{ GeV}^{-4} , \quad (7.22)$$

with the error taken from the range of different analyses. Again, there have to be substantial $\mathcal{O}(q^6)$ contributions, the electromagnetic corrections are small and will lead only to small modifications in the analysis of the $\mathcal{O}(q^6)$ counterterms.

We now turn to the neutral pions. Here, the only effect is due to the pion mass difference in the pion loops, see fig. 9. The corresponding contribution to the radius takes the form

$$\langle r^2 \rangle_{\pi^0,\text{mass}}^S = -\frac{12}{(4\pi F)^2} \log \frac{M_{\pi^\pm}}{M_{\pi^0}} + \left(\frac{e}{4\pi}\right)^2 \frac{2Z}{M_{\pi^\pm}^2} . \quad (7.23)$$

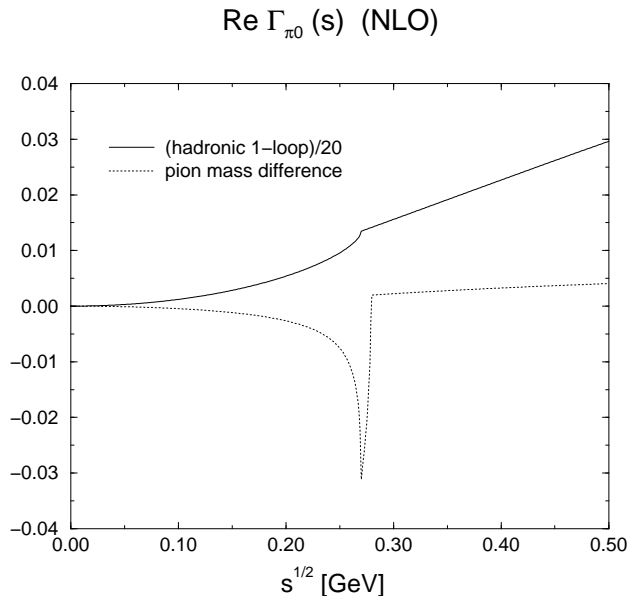


Figure 9: Scalar form factor of the neutral pions in the time-like region. The only electromagnetic contribution is due to the pion mass difference. It is shown in comparison with the strong fourth order contribution. The latter is divided by a factor of 20.

Numerically we have

$$\langle r^2 \rangle_{\pi^0, \text{mass}}^S = -0.0094 \text{ fm}^2, \quad (7.24)$$

using $M_{\pi^0} = 134.97 \text{ MeV}$. This amounts to a 2% reduction of the hadronic result. Such an enhancement of the electromagnetic effects for the neutral particles as compared to the charged ones has also been observed in pion-nucleon scattering [15, 16, 17, 18] or neutral pion photoproduction off nucleons [34]. Finally, we study the normalization. We find

$$\tilde{\Gamma}_{\pi^0}(0) = M_{\pi^0}^2 (1 - 0.013 - 0.004 - 0.001), \quad (7.25)$$

where the first correction is due to the hadronic shift [1], the second one is due to the strong isospin breaking $\sim \bar{l}_7$ (we use $\bar{l}_7 = 1.0$), and the third term stems from the pion mass difference in the loops. We note that the strong isospin breaking amounts to a 30% correction of the strong isospin conserving shift.

To conclude this section, let us quote the result for the isospin-breaking one-loop contribution to the parameter $c_{\pi^0}^S$,

$$c_{\pi^0, \text{mass}}^S = \frac{1}{(4\pi F)^2} \frac{1}{M_{\pi^\pm}^2} \left(\frac{1}{6} - \frac{3}{20} \frac{M_{\pi^\pm}^2}{M_{\pi^0}^2} - \frac{1}{60} \frac{M_{\pi^0}^2}{M_{\pi^\pm}^2} \right) = -0.35 \text{ GeV}^{-4}, \quad (7.26)$$

which is again slightly larger than for the charged pions, but small compared to the two-loop contribution.

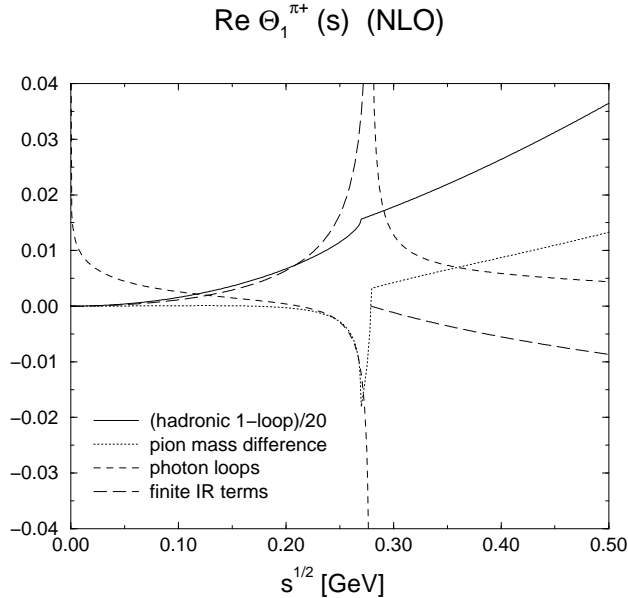


Figure 10: Normalized form factor $\Theta_1^{\pi^\pm}(s)$ of the energy–momentum tensor for charged pions. The various electromagnetic corrections are shown in comparison with the strong fourth order contribution. The latter is divided by a factor of 20.

7.3 Form factors of the energy–momentum tensor

We have calculated the various form factors of the energy–momentum tensor for charged and neutral pions discussed in sect. 5. We refrain from discussing all of them in detail but rather show two typical cases. $\Theta_1^{\pi^\pm}(s)$ is given in fig. 10. The electromagnetic corrections look similar to the ones for the scalar form factor shown in fig. 8 with two notable exceptions. First, as noted before, the photon loop corrections diverge at $s = 0$, and second, the corrections due to the pion mass difference in the pion loops grow with increasing s after the two–pion threshold. The tensor form factor for charged pions is shown in fig. 11. In this case, the hadronic fourth order correction is simply a polynomial linear in s since there are no loop contributions. The size of the electromagnetic corrections is typically a few percent of the strong fourth order contribution, with the exception of the kinematical points where divergences appear. Finally, we note that the form factors of the trace of the energy–momentum tensor are very similar to the scalar form factors discussed in the previous paragraph.

8 Summary

In this paper, we have considered various pion form factors in the presence of virtual photons at next–to–leading order in $SU(2)$ chiral perturbation theory. The pertinent results of this investigation can be summarized as follows:

- (1) The vector form factor of the pion has been calculated including photon loops and

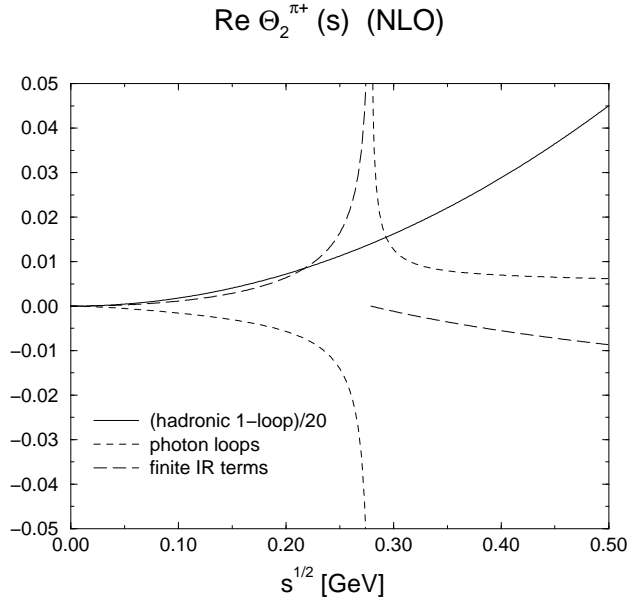


Figure 11: Tensor form factor of the energy–momentum tensor for charged pions. The various electromagnetic corrections are shown in comparison with the strong fourth order contribution. The latter is divided by a factor of 20.

electromagnetic counterterms. The electromagnetic corrections are typically a few percent of the strong fourth order contribution, cf. figs. 6, 7. The intrinsic virtual photon corrections to the pion charge radius is of the order of 1%. In addition, there is a detector resolution dependent contribution to the radius which is of the order of 5% for $\Delta E = 10 \dots 20$ MeV. We have discussed how to deal with this contribution.

- (2) We have also investigated the scalar form factor of the charged and the neutral pions. For the charged pions, the results are similar to the vector form factor, cf. fig. 8. For neutral pions, the only effect is due to the pion mass difference in the pion loops. This leads to a 2% reduction of the scalar radius of the neutral pion. We have also found that the scalar form factors at zero momentum transfer are more strongly affected by isospin breaking.
- (3) The pion matrix elements of the energy–momentum tensor are parametrized by a scalar and a tensor form factor. We have extended the chiral Lagrangian coupled to gravity in the presence of virtual photons. There is only one additional electromagnetic operator at fourth order. Since the energy–momentum tensor can couple directly to virtual photons, one of the corresponding form factors shows a divergence at zero momentum transfer not present in the scalar form factor of the pion. Typically, electromagnetic corrections are small, see figs. 10, 11.

We conclude by noting that presently the largest uncertainty in the low energy representation of the pion form factors is due to the uncertainties in the low energy constants \bar{l}_4 and \bar{l}_6 .

Strong two-loop corrections or the virtual photon effects calculated here are sizeably smaller.

Acknowledgements

We are grateful to K. Melnikov for pointing out an error in the previous version.

References

- [1] J. Gasser and H. Leutwyler, Ann. Phys. (NY) 158 (1984) 142.
- [2] S. Weinberg, Physica 96A (1979) 327.
- [3] U. Bärger, Phys. Lett. B377 (1996) 147; Nucl. Phys. B479 (1996) 392.
- [4] J. Gasser and Ulf-G. Meißner, Nucl. Phys. B357 (1991) 90.
- [5] J. Bijnens, G. Colangelo, and P. Talavera, JHEP 9805 (1998) 014.
- [6] J. Bijnens et al., Phys. Lett. B374 (1996) 210; Nucl. Phys. B508 (1997) 263.
- [7] M. Knecht et al., Nucl. Phys. B457 (1995) 513 .
- [8] S. Eidelman and F. Jegerlehner, Z. Phys. C67 (1995) 585;
R. Alemany, M. Davier, and A. Hocker, Eur. Phys. J. C2 (1998) 123.
- [9] Ulf-G. Meißner, G. Müller, and S. Steininger, Phys. Lett. B406 (1997) 154;
(E) *ibid* B407 (1997) 434.
- [10] M. Knecht and R. Urech, Nucl. Phys. B519 (1998) 329.
- [11] J.F. Donoghue, B.R. Holstein, and D. Wyler, Phys. Rev. D47 (1993) 2089.
- [12] J. Bijnens, Phys. Lett. B306 (1993) 343.
- [13] R. Urech, Nucl. Phys. B433 (1995) 234.
- [14] G. Ecker, J. Gasser, A. Pich, and E. de Rafael, Nucl. Phys. B321 (1989) 311.
- [15] S. Weinberg, Trans. N.Y. Acad. of Sci. 38 (1977) 185.
- [16] Ulf-G. Meißner and S. Steininger, Phys. Lett. B419 (1998) 403.
- [17] N. Fettes, Ulf-G. Meißner, and S. Steininger, Phys. Lett. B451 (1999) 233.
- [18] G. Müller and Ulf-G. Meißner, Nucl. Phys. B556 (1999) in print.
- [19] M. Ademollo and R. Gatto, Phys. Rev. Lett. 13 (1964) 264.
- [20] J.F. Donoghue and H. Leutwyler, Z. Phys. C52 (1991) 343.
- [21] J.F. Donoghue, J. Gasser, and H. Leutwyler, Nucl. Phys. B343 (1990) 341.
- [22] S. Raby and G. West, Phys. Rev. D38 (1988) 3488; *ibid* D39 (1989) 828.
- [23] H. Leutwyler and M. Shifman, Phys. Lett. B221 (1989) 384.

- [24] V.A. Novikov and M.A. Shifman, *Z. Phys.* C8 (1981) 43;
M. Voloshin and V. Zakharov, *Phys. Rev. Lett* 45 (1980) 688.
- [25] S. Bellucci, J. Gasser, and M.E. Sainio, *Nucl. Phys.* B423 (1994) 80;
(E) *ibid* B431 (1994) 413.
- [26] J. Bijnens and J. Prades, *Nucl. Phys.* B490 (1997) 239.
- [27] B. Moussallam, *Nucl. Phys.* B504 (1997) 381.
- [28] R.P. Feynman, *Phys. Rev.* 56 (1939) 340.
- [29] H. Hellman, *Einführung in die Quantenchemie*, Deuticke Verlag, Leipzig (1937).
- [30] L.S. Brown, *Quantum Field Theory*, Cambridge University Press (1992).
- [31] S. Weinberg, *The Quantum Theory of Fields*, Vol.1, Cambridge University Press (1995).
- [32] F.S. Roig and A.R. Swift, *Nucl. Phys.* B104 (1976) 533.
- [33] H.B. O'Connell et al., [hep-ph/9707404](#).
- [34] V. Bernard, N. Kaiser, and Ulf-G. Meißner, *Z. Phys.* C70 (1996) 483.